Sudan University of Science and Technology
College of Graduate Studies

Modeling of PID Controller for an Auto-Pilot Aircraft Pitch Control

نمذجة المتحكم التناسبي التكاملي التفاضلي للتحكم في محور الانحدار للطيار الآلي

A thesis Submitted in Partial Fulfilment of the Requirement for the Degree of M.Sc. in Mechatronics Engineering

Prepared By:
Omar Mohamed Osman Alradi Mokhtar

Supervisor:
Dr. Ebtihal H. G. Yousif

August 2022

الإستهلال

بِسْمِ اَللَّهِ اَلرَّحْمٰنِ اَلرَّحِيمِ

(اَللَّهُ نُورُ اَلسَّمَاوَاتِ وَالْأَرْضِ مَثَلُ نُورِهِ كَمِشْكَاةٍ فِيهَا مِصْبَاحٌ اَلْمِصْبَاحُ فِي زُجَاجَةٍ اَلزُّجَاجَةُ كَأَنَّهَا كَوْكَبٌ دُرِّيٌّ يُوقَدُ مِنْ شَجَرَةٍ مُّبَارَكَةٍ زَيْتُونِةٍ لَّا شَرْقِيَّةٍ وَلَا غَرْبِيَّةٍ يَكَادُ زَيْتُهَا يُضِيءُ وَلَوْ لَمْ تَمْسَسْهُ نَارٌ نُّورٌ عَلَى نُورٍ يَهْدِي اَللَّهُ لِنُورِهِ مَنْ يَشَاءُ وَيَضْرِبُ اَللَّهُ اَلْأَمْثَالَ لِلنَّاسِ وَاللَّهُ بِكُلِّ شَيْءٍ عَلِيمٍ)

سورْهْ اَلْنور،الايهْ (٣٥)

Dedication

To the candle that lit my way from the pride of darkness..

To the lips that prayed more for us..

To whom I planted a love to know in my heart..

To my mother, may God take care of her..

TO departed from life and live in my arms..

To my father, may God have mercy on him..

To those who entered my life..

And with them, we have hope in life..

To my wife and son.....

To the eyes that saw hope in us whenever we looked..

To the hearts that wanted us proud..

To my brothers and family..

I give unrestricted advice and admission to my teachers..

To evacuate my teachers..

You are my companion and forget, and honesty does not reward me with loyalty..

To the companions of the trail.....

TO tall, you have the right of love and affiliation in my blood..

To home.....

Acknowledgments

First of all thanks for my God who helped me to complete this project. I would like to express my deepest appreciation to my supervisor Dr. Ebtihal Haider Gismalla Yousif for all her assistance during this master thesis work , and everybody help me to success of this research.

Abstract

An aircraft contains three rotational motions like pitch, yaw and roll. The pitch motion is controlled by the elevators that are present on the part of the tail, at the rear of an aircraft. An autopilot is a software or tool that can only manage the aircraft under certain conditions using the vehicle's hydraulic, mechanical and electronic systems. This system, which can follow the flight plan, can stabilize speed and height as well as the location of the front of the aircraft (heading). Pilots mostly lead the aircraft in a controlled manner by autopilot except for departure and landing. Autopilot is mostly used on passenger aircrafts. In this research, elevators are considered as plant and its transfer function is used in modeling of the controller. The proportional integral derivative (PID) controller was used in the modeling of the control system to find the best performance for the aircraft (pitch motion). The comparison was made before and after adding the PID controller and the performance parameters are as follows. Before adding the controller, the rise time was 0.285s, the peak time was 0.143s, the settling time was 0.914s, the overshoot was 137 and the steady state error was. 0.065. After adding the PID controller it was found that at the selected point (-3.7915-0.0466i), from the geometric locus of the roots, achieves the best performance of the aircraft (pitch motion). The rise time is 0.0021s, the peak time is 0.0045s, the settling time is 0.0124s, the overshoot is 8.6561 and the steady state error is zero. It's noted from comparison that adding the PID controller led to better performance for the aircraft in terms of the stability which the required in flight until we reach safe and comfortable flight and fewer accidents.

المستخلص

تحتوي الطائرة على ثلاث حركات دورانية مثل الانحراف والانعراج والدوران. يتم التحكم في حركة الانحدار بواسطة المصاعد الموجودة على جزء الذيل ، في الجزء الخلفي من الطائرة. الطيار الآلي هو برنامج أو أداة يمكنها فقط إدارة الطائرة في ظل ظروف معينة باستخدام الأنظمة الهيدروليكية والميكانيكية والإلكترونية للمركبة. يمكن لهذا النظام ، الذي يمكنه اتباع خطة الطيران ، أن يثبّت السرعة والارتفاع بالإضافة إلى موقع مقدمة الطائرة (العنوان). يقود الطيارون في الغالب الطائرة بطريقة خاضعة للرقابة بواسطة الطيار الآلي باستثناء الاقلاع والهبوط. يستخدم الطيار الآلي في الغالب على طائرات الركاب. في هذا البحث ، تعتبر المصاعد مصنعا ويتم استخدام وظيفة النقل الخاصة بها في نمذجة وحدة التحكم. تقوم وحدة التحكم التناسبي التكاملي التفاضلي المصممة على غرار أداء حركة خطوة أفضل مع استقرار جيد.تم استخدام المتحكم التناسبي التكاملي التفاصلي في تصميم المتحكم لايجاد افضل اداء ممكن للطائرة . عند المقارنه بين نتائج الاداء قبل وبعد ادخال المتحكم وجد ان نتائج اداء الطائره قبل ادخال المتحكم هي (زمن الصعود = ٠,٢٨٥ ثانية ،وزمن الذروة = ٠,١٤٣ ثانية ، وزمن الاستقرار =٠,٩١٤ ثانية ،والتجاوز = ١٣٧ ، وخطأ الحالة المستقرة = ٠,٠٦٥) اما عند ادخال المتحكم وجد افضل اداء للطائره عند النقطه المختاره من المحل الهندسي للجذور (-٣,٧٩١٥-٠,٠٤٦٦ت) كانت النتائج كالاتي (زمن الصعود = ٠,٠٠٢١ ثانية ،وزمن الذروة = ٠,٠٠٤٥ ثانية ، وزمن الاستقرار =٠,٠١٢٤ ثانية ،والتجاوز = ٨,٦٥٦١ ، وخطأ الحالة المستقرة = صفر). يلاحظ عند المقارنه انه بعد ادخال المتحكم التناسبي التكاملي التفاضلي وجد ان نتائج اداء الطائره افضل ادت الي تحسين الاستقراريه وهي من المتطلبات الاساسيه في عملية الطيران حتي نحقق طيران امن ومريح مع التقليل من الحوادث .

Table of Contents

List of Figures

List of Tables

List of Abbreviations

PID	Proportional–Integral–Derivative
c.g	Center of Gravity
NF	Natural Frequency
DM	Damping Ratio
SSE	Steady State Error
Kc	Crossover gain
Wc	Critical frequency
PT	Peak Time
RT	Rise Time
ST	Setteling Time

List of Symbols

$f(x, y)$	pixel value as a function of x (row index) and y (column index)
M	number of row
N	number of columns
Kd, Ki, Kp	parameters of PID Controller

Chapter one
Introduction

1.1 Overview

After the successful development of man-carrying airplane by Wright brothers, the development of auto-pilots emerged. The first auto-pilot (or) automatic flight controller in the world is designed by the Sperry brothers in 1912. Currently, the auto-pilot design relies heavily on automatic control systems to monitor and control the aircraft subsystems [1]. Generally, an aircraft is controlled by three main control surfaces. They are elevator, rudder, and ailerons. These three control surfaces are used to control pitch, yaw and roll actions of an aircraft respectively [1].

Elevator, rudder and ailerons are depicted in fig. 1. Pitch control is achieved by changing lift. Yaw control is achieved by deflecting a flap on vertical tail called rudder and roll control can be achieved by deflecting small flaps present toward the wing tips in differential manner and these are called ailerons. The two ailerons are typically interconnected and both ailerons move in opposite direction to each other. The pitching motion is being caused by the deflection of the elevator of this aircraft. The elevator is a hinged section at the rear of the horizontal stabilizer. There is usually an elevator on each side of the vertical stabilizer. The elevators work in pairs; when the right elevator goes up, the left elevator also goes up. The pitching motion of an aircraft is controlled by adjusting the pitch angle with the use of elevators. Pitch angle control is a longitudinal problem and this work is developed to control the pitch angle of an aircraft for pitch control in order to stabilize the system, when an aircraft performs the pitching action [2].

The first aircraft autopilot was developed by Sperry Corporation in 1912. The autopilot connected a gyroscopic Heading indicator and attitude indicator to hydraulically operated elevators and rudder (ailerons were not connected as wing dihedral was counted upon to produce the necessary roll stability.) It permitted the aircraft to fly straight and level on a compass course without a

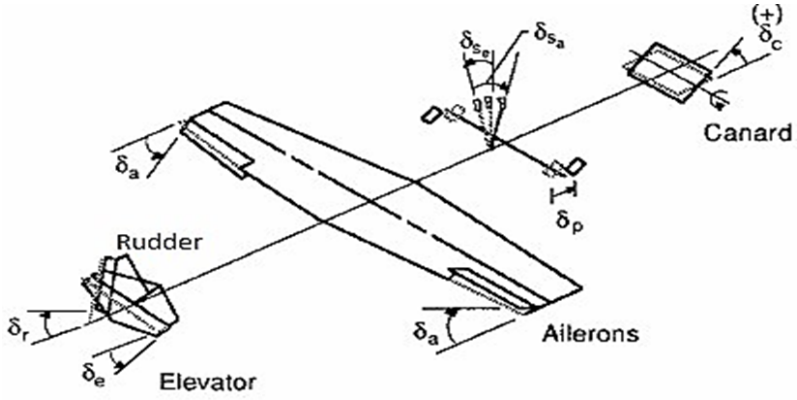

Figure 1.1: Controls of an aircraft [Showing elevators, rudder, ailerons]

pilot's attention, greatly reducing the pilot's workload [3]. Lawrence Sperry (the son of famous inventor Elmer Sperry) demonstrated it two years later in 1914 at an aviation safety contest held in Paris. At the contest, Lawrence Sperry demonstrated the credibility of the invention were shown by flying the aircraft with his hands away from the controls and visible to onlookers of the contest. This autopilot system was also capable of performing take-off and landing, and the French military command showed immediate interest in the autopilot system. Wiley Post used a Sperry autopilot system to fly alone around the world in less than eight days in 1933. Further development of the autopilot were performed, such as improved control algorithms and hydraulic servomechanisms. Also, inclusion of additional instrumentation such as the radio-navigation aids made it possible to fly during night and in bad weather. In 1947 a US Air Force C-53 made a transatlantic flight, including takeoff and landing, completely under the control of an autopilot. In the early 1920s, the Standard Oil tanker J.A Moffet became the first ship to use an autopilot [4].

1.2 Problem Statement

The flight process requires high stability so as not to lead to disasters, the least disaster can lead to the loss of many lives, so improvement in stability continues until we reach the best possible stability .

1.3 Proposed Solution

Designing a control system that improves the stability system that was previously designed by proportional controller, which gave unstable performance by using the PID Controller.

1.4 Objectives

To achieve a better response, more stable with less ringing and settling time, with some considerable overshoot To reach safer and more comfortable flying and reduce accidents as little as possibl.

1.5 Methodology

- Study and find mathematical model
- Mathematical model analysis
- Determine system stability
- Design control system by PID controller

Chapter Two
Background And Related Work

2.1 Autopilot

An autopilot is a device used to guide an aircraft without direct assistance from the pilot. Early autopilots were only able to maintain a constant heading and altitude, but modern autopilots are capable of controlling every part of the flight envelope from just after take-off to landing. Modern autopilots are normally integrated with the flight management system (FMS) and, when fitted, the autothrottle system.

Autopilot software, which is integrated with the navigation systems, is capable of providing control of the aircraft throughout each phase of flight. If an autothrottle/autothrust system is installed, the appropriate thrust may be automatically set during take-off, and is then adjusted automatically as the climb progresses, while the aircraft climbs at the appropriate speed for its mass and ambient conditions. The aircraft then levels at the required altitude or flight level while the power is adjusted to achieve and maintain the programmed speed. At the same time, the aircraft follows the flight plan route. If an autothrottle is not installed, the pilot must make all power adjustments appropriate to the autopilot mode and phase of flight.

On commencing the descent, the power is adjusted and the aircraft descends at the appropriate speed and on the required routing, leveling as required in accordance with the flight clearance until the approach is commenced. If this is to be a Category III Instrument Landing System (ILS) approach with Autoland, the autopilot controls the aircraft flight path so that it follows the ILS glide path and localiser, adjusting the power to maintain the appropriate speed and commencing the flare as required to achieve a safe landing without the runway being visible until the final stage of the approach. On some aircraft, the autopilot can then guide the aircraft so that it maintains the runway centre-line until it stops.

At any stage of the flight, the pilot can intervene by making appropriate

inputs to the autopilot or the FMS. In an emergency, the pilot can disengage the autopilot and take over manual control, usually by pressing a switch mounted conveniently on the control column (although alternative means of disengaging the autopilot are available). Modern aircraft have another switch or throttle position which allows the pilot to change instantly from approach to go-around mode if necessary. If the aircraft is not fitted with an automatic go-around function, pilots must disconnect the autopilot and fly the missed approach manually.

The safe and efficient operation of automatic systems relies on clear understanding of the capabilities and the design philosophy of the equipment. Failure to achieve this level of understanding has resulted in several fatal accidents.

2.1.1 Wing Levelers

The most straightforward systems are called wing levelers.As the name suggests, they have only one function–to keep the wings level.Even this is usually sufficient to reduce a significant portion of the pilot's Wing levelers are useful only when the pilot is very good at getting an airplane trimmed for level flight.With the elevator trim tab's help, most planes require very little input to remain at altitude.Roll requires more correction, however, so a wing leveler can come in handy.

2.1.2 Two-Axis Systems

Two-axis systems provide a lot more options and a lot more hands-off flying time for the pilots. They also offer the ability to be coupled with some types of instrument approaches.

Notice that neither system controls the airplane's rudder. Since the rudder requires very little input during cruise flight anyway, it's not worth the expense and effort of adding the control to the rudder pedals.

Most pilots will be resting their feet on the pedals regardless of whether or not the autopilot is on. Applying a little bit of rudder pressure will be their natural reaction, whether the computer or the pilot rolls into the turn.There are three-axis systems out there, but they're usually reserved for airliners and large transport-category aircraft.

2.1.3 Roll and Pitch Control

To control roll, a servo motor is mounted that moves the control stick or wheel inside the aircraft. The autopilot controls the roll of the aircraft with the ailerons, just like the pilot would.

The pitch of the plane is controlled via the trim tab. Since the trim tab moves the larger elevator, this is an easy indirect way to control pitch without having to make a mechanical linkage to move the control yoke.

Autopilot-equipped aircraft usually also have electric trim wheels. A servo motor will spin the trim wheel up and down. This system is how the autopilot controls the aircraft's pitch, but the pilot can also use the electric trim during normal flight.

Electric trim is nice to have on any plane. It means that the pilot can simply move a toggle switch with their thumb, right on the control wheel, instead of moving the much larger trim wheel. The trim wheel is still there, and it can be moved manually if desired.

2.1.4 Two Vital Componentsl

There are two vital components to any autopilot system in the cockpit. One is a disconnect switch. It's so important that it is usually located right on the control wheel at the pilot's thumb. It can be deactivated with a second's notice. Another important control is the circuit breaker that will disconnect all power from the autopilot system.

Why are these safety cutoff features important? Autopilots are computerized systems that can–and do sometimes–go haywire. The pilot needs to be able to disconnect the system and take over manually flying the plane in an emergency. If the autopilot starts acting unexpectedly or putting the aircraft into a dangerous flight attitude, the pilot needs to be able to take immediate action.

Electric trim systems have been known to enter runaway situations, where the button gets stuck or the wiring shorts out. In this case, the plane will pitch up or down dangerously. Pulling the circuit breaker for the autopilot system will remove all power from the trim as well.

2.1.5 Autopilot Basic Modes of Operation

2.1.5.1 ROLL Mode

An autopilot's most basic mode is "ROLL," which keeps the wings level. Most units can also hold a heading (HDG) or a navigational radio course (NAV).

2.1.5.2 Heading Hold Mode (HDG)

The heading hold mode is controlled by a settable bug on the directional gyroscope. This instrument is right in front of the pilot, and it's where the pilot would look to figure out their heading anyway. The pilot sets the heading they want to fly, and the autopilot will track that heading if the HDG mode is selected.

2.1.5.3 Navigational Mode (NAV)

The navigation function gives the autopilot a lot more authority. It is usually tied to the NAV1 indicator, so whatever navigational radios work there will be coupled into the autopilot. On most aircraft, this includes the first VOR navigation radio and the GPS. Whatever course the pilot has selected there, the autopilot will keep centered.

2.1.5.4 Combined

The two modes can be combined for simple flight tasks. For example, it's not uncommon for a plane to be given a heading to fly until they can join a VOR course. In this case, the autopilot can be operated in HDG mode with the NAV mode armed. The autopilot will watch the navigational course, and as it comes into view, it will command a slow turn to join that course.

If a two-axis autopilot is installed, it holds its altitude based on an altitude that the pilot sets. ALT mode indicates that the autopilot will hold that altitude. Since the autopilot's altimeter is built-in and not the one used by the pilot, the current barometer setting must be input to the autopilot as well. These systems are usually advanced enough to allow the pilot to change altitudes without touching the flight controls. If a descent is desired, then the pilot changes the selected altitude on the autopilot. The autopilot then switches into a vertical speed hold mode, which the pilot can fine-tune to their

liking. The computer arms the ALT hold mode and waits until it reaches the selected altitude, where it levels off.

Of course, during the level-offs, the autopilot cannot change the throttle setting. So the pilot must still make power adjustments, just like they must still make rudder inputs.

2.1.6 Flight Management System (FMS)

More technically advanced aircraft have some form of a system known as FMS, or flight management system.

On airliners and transport-class airplanes, the FMS is usually the primary location where pilots input their navigational planning. The FMS is tied to all other systems, so ideally, it simplifies the use of multiple navigational services while in the air. It talks to the GPS unit, the VOR radios, the ADF radio, and the INS (inertial navigation system) if installed. All of this makes a powerful unit that gets a lot of pilot attention. But the primary function of FMS is to layout the flight course in advance. If your flight path takes you over the ABC VORTAC, then the XYZ VORTAC, and then to intercept the I-ILS instrument approach, the computer can be set up to do all of those things before the plane even takes off.

That capability is found in many aircraft today, even light aircraft. Modern GPS systems and glass cockpits allow the pilot to have FMS-like control over the plane's course. The result is that a course line is predefined in the computer systems before departure, which reduces workload from the pilot and enables them to use the autopilot to fly that course.

2.1.7 Automation Management Training

If all of this sounds more like computer programming and less like flying an airplane, you'd be right. All of this head-down time comes at a price for pilots, who now have a lot more to do inside the cockpit.

The art of dealing with all of the fancy computers, autopilots, and FMS systems is known as automation management. It's now a vital skill for pilots to build.

It might seem to a non-flyer that pilots must be very good at multitasking and dividing their attention. But research has shown that the human brain is extremely bad at multitasking. We think we are good at dividing our attention

equally, but what really happens is that we are not focused on anything very well. Pilots know their limits, and while it may look like they're multitasking, what they are doing is effectively managing their time. When workload is light, like on the ground before departure or during quiet cruise flight, they are preparing for busy parts of the flight they know are coming.

In the end, this is the beauty of autopilot. The pilot must still monitor an autopilot system at all times. But they do not have to make the control adjustments for every gust of wind or every course change. That frees up some of their mental resources to deal with other issues. If you see a pilot with their head down programming a computer or dealing with the FMS, chances are they are preparing for an upcoming phase of flight when they know they will be task saturated. For example, takeoffs, departures, approaches, and landings are times when they will have too much to do and cannot spare the attention required to mess with the computers.

2.1.8 How Much of a Flight is on Autopilot?

On a commercial airliner, nearly the entire flight is flown on autopilot. The pilots continuously monitor the computer to ensure that it follows the correct programmed course and make sure that all of the programming is in order.

Autopilot systems cannot takeoff, so taxi, takeoff, and other ground operations are done manually. The autopilot is usually engaged a few hundred feet off of the runway after departure.

When arriving at an airport, the autopilot is usually used until the very last segment of the approach. When the runway is in sight, the pilot flies the plane to the landing.

2.1.9 Do Airplanes Land on Autopilot?

Some planes do have autoland systems, but these are generally only used in poor visibility when they must be used. With a certified autopilot, some airplanes can land after an instrument approach in zero-visibility conditions.

2.2 PID Controller

The PID integrated proportional controller is the most common type in the civil industry, where 95% of the problems can be solved using it, and some

companies produce it as a stand-alone unit or combine it with some systems such as temperature control. This ruler has gone through many stages of development as relays and motors began Synchronous or hydraulic, followed by the use of electronic circuits, and finally it became possible to implement this method of control using a microprocessor. Many manufacturers of control devices have begun to take an interest in this ruler, so that it has the ability to self-adjust, whether it is using prepared tables or using adaptive control methods. Despite the widespread use of a PID ruler, its control is often not optimal due to the difficulty of setting three parameters together [5].

2.3 Effect of PID Control Transactions

The effect of each PID arbitrator component on the control system can be summarized in general as follows:

1. The proportional component decreases the steady-state error and increases the maximum output transient value.

2. The integral component eliminates the error during the stabilization phase, but it causes an increase in oscillations and their amplitude during the transient phase and may lead in certain conditions to a loss of equilibrium for the system as a whole. It is noticed that the integration element can be dispensed with if the original system already contains an integration relationship.

3. The differential component reduces vibrations and amplitude during the transient phase, but it is sensitive to lust and sudden changes in the base signal

4. It is difficult to make general provisions about the relationship between the elements of the ruler and the time of stability, as this depends on the size of the system and the locations of the roots of the numerator and denominator in the vector function.

The effect of PID controller parameters on closed-loop performance is shown in Table 2.1.

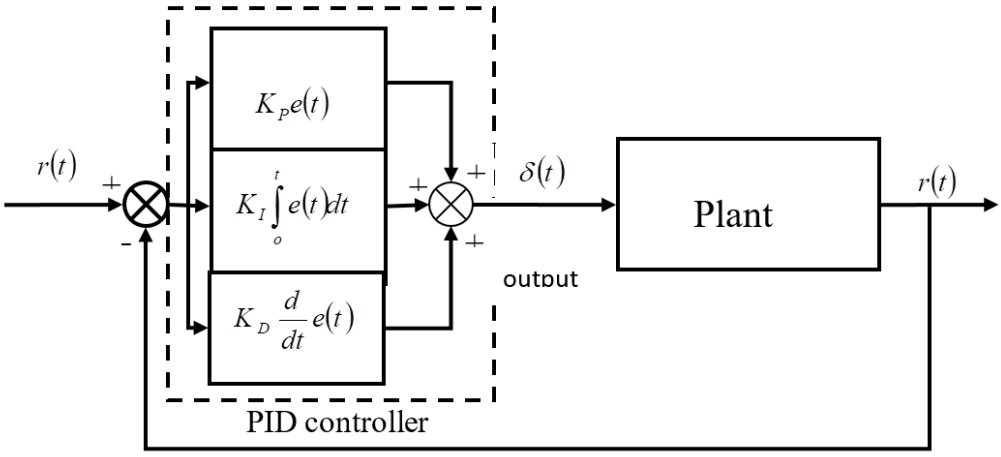

Figure 2.1: PID control system with a feedback

Table 2.1: Effect of PID Controller Parameters on Closed-Loop Performance

controller	Rise Time	Overshoot	Settling Time	Steady State Error
K_p	Decrease	Increase	Small Change	Decrease
K_I	Decrease	Increase	Increase	Eliminate
K_D	Small Change	Decrease	Decrease	Small Change

2.4 Transformational Function of the PID Controller

The figure 2.1 shows a PID control system with a feedback

Stability and good control is by the following equation:

$$\delta(t) = K_p \left[e(t) + \frac{1}{T_I} \int_0^t e(\tau)d\tau + T_d \frac{d}{dt} e(t) \right] \tag{2.1a}$$

$$= K_p e(t) + K_I \int_0^t e(\tau)d\tau + K_d \frac{d}{dt} e(t) \tag{2.1b}$$

The transforming function of the PID controller is given by the following equation:

$$\delta(s) = K_P + \frac{K_I}{s} + K_D s \tag{2.2}$$

2.5 Tuning Techniques

That is, how do we place the coefficients K_d, K_i, K_p at a certain level to eliminate the decline between desired input and output Actual, and there are

three techniques to fine-tune this controller are trial and error techniques, analytical techniques and experimental techniques.

2.5.1 Trial and Error Technique

The algorithm for this method is as follows:

1. Get the open loop response and decide what improvement is needed.
2. Addition of a proportional controller to reduce rise time.
3. Addition of a differential controller to reduce vibration.
4. Add an integral controller to remove the steady-state error.
5. Repeat the previous steps if necessary.

2.5.2 Analytical Techniques

It contains a form linking the current position and the current rate of change.

2.5.3 Experimental Techniques

There are several experimental techniques, but the most used is the Ziegler-Nichols technique and it is used for its simplicity and application.

2.6 Ziegler-Nichols Method

2.6.1 Closed Loop Method Algorithm

1. Enable proportion work by making K_i and K_d zero.
2. Increase the proportion gain even the output of the system is subjected to constant vibrations.
3. From the graph determine the final period of P_u
4. Calculate parameters according to the schedule.
5. Apply the parameters specified in paragraph 4 and perform a simulation of the closed-loop performance test.

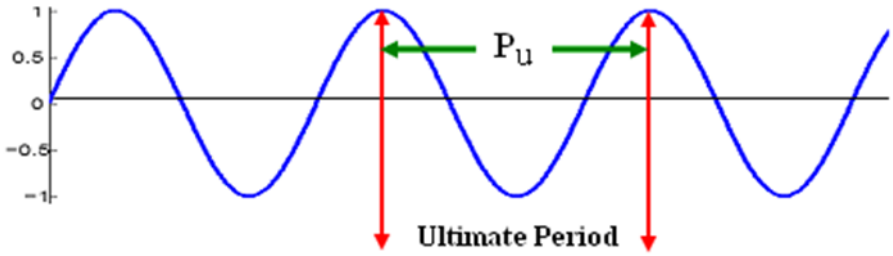

Figure 2.2: Diagram of closed loop method

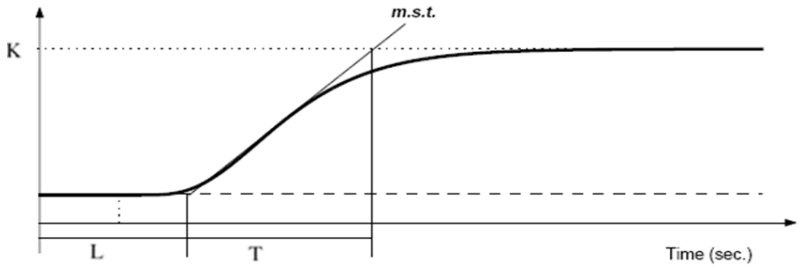

Figure 2.3: Diagram of open loop method

Table 2.2: PID parameter- (closed loop)

controller	K_p	T_I	T_D
P	$0.5\ K_u$	∞	0
PI	$0.45\ K_u$	$\frac{1}{1.2}P_u$	0
PID	$0.6K_u$	$0.5P_u$	$0.125P_u$

2.6.2 Open loop method

Open loop techniques can be divided into two methods, the reaction curve method and the roots Lucas method:

2.6.2.1 Reaction curve method

This is based on information gained from the open loop step Function transformation:

$$G_p(s) = \frac{K^{-Ls}_{e}}{Ts+1} \tag{2.3}$$

Algorithm

1. Apply the input step to the open loop and adjust the gain (K), time delay (L) and time constant (T) until the response is as close as possible

to the original plant.

2. Determine the parameters (T, L, K).

3. Calculate the parameters according to Table 2-3.

4. Apply the parameters in pragraph 3 and perform a simulation of the closed-loop performance test.

Table 2.3: PID parameters (open loop - Reaction curve)

controller	K_p	T_I	T_D
P	$\frac{K}{L}$	∞	0
PI	$0.9\ \frac{K}{L}$	$\frac{T}{0.3}$	0
PID	$1.2\frac{K}{L}$	$0.5L$	$2L$

2.6.2.2 The roots locus method

This theory is based on the information we obtain from the location of the open-loop roots [6]

Algorithm

1. Plot the location of the segments for the open loop system.

2. From the position of the strips, we obtain the following information: the gain, Kc, and the critical frequency, Wc.

3. From the frequency Wc, we calculate the cycle Tc.

4. Put the values of Kc and Tc in following Table to calculate the parameters.

Table 2.4: PID parameters(open loop - Root locus) .

controller	K_p	T_I	T_D
PID	$0.6K_c$	$0.5T_c$	$0.125T_c$

Chapter Three
Mathematical Model

Due to the high costs of conducting practical tests on a real plane, it was necessary to think of a way to conduct these tests, hence the idea of building a mathematical model.

3.1 Reference Frame

To find the mathematical model for the aircraft under study, one must first define and understand some of the reference frames on which the mathematical model is built [7]. Kinetic reference frames can be divided into:

3.1.1 Inertial Frame

It is the frame, in which Newton's law of motion is used, and the origin of this frame is placed in a suitable place on the surface of the earth, and from the following figure we note that the axes of this frame are as follows: The X-axis points to the North of the Earth. YE axis points perpendicular to XE and points east. The ZE axis is perpendicular to the XE - YE plane and points towards the center of the globe.

3.1.2 Body Frame

This frame is attached to the plane and its origin is placed in the center of gravity of the plane c.g. From the following figure, we find that the axes of this frame are as follows:

The XB axis is identical to the longitudinal axis of the plane.

The YB axis is orthogonal to XB and points to the right wing of the aircraft.

The ZB axis is orthogonal to the XB - YB plane and points to the bottom of the plane.

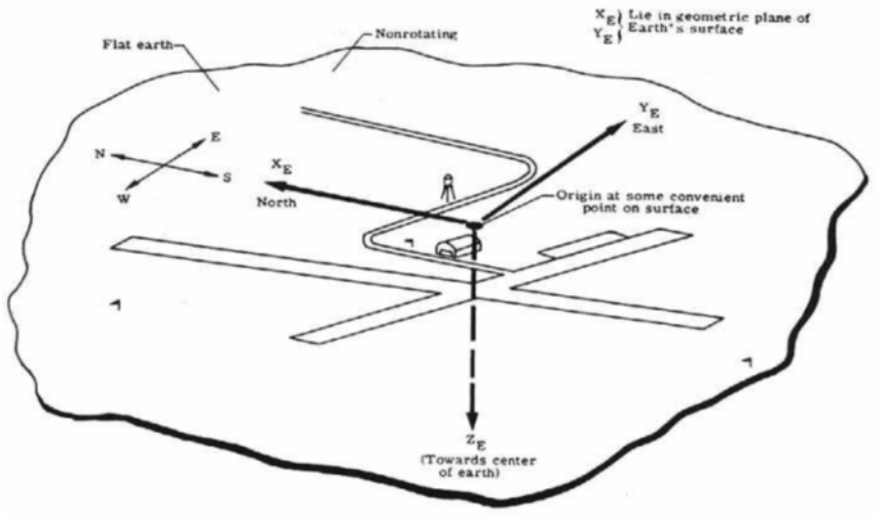

Figure 3.1: Inertial Frame

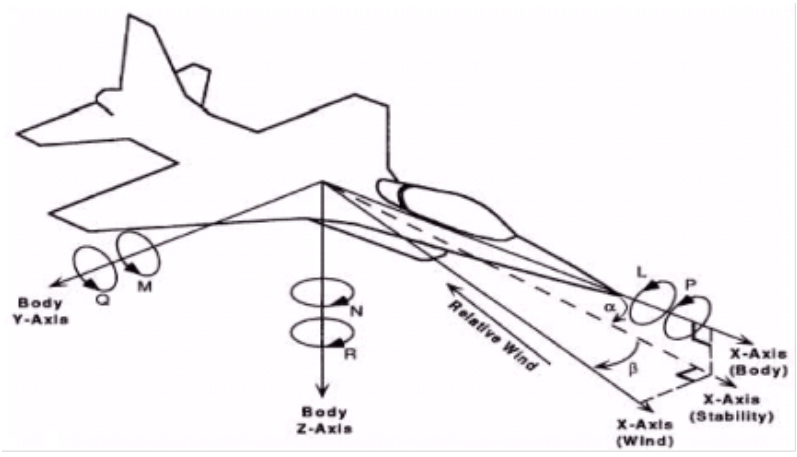

Figure 3.2: shows the body frame and stabilization

3.1.3 Stability Frame

This frame is the same as the body frame when the XB axis applies to the plane's velocity vector in flight. It is used to simplify the aerodynamic calculations as in the previous figure.

Flight vectors in Cartesian coordinates are written as follows:

$$V_B = Ui_B + Vj_B + Wk_B \tag{3.1}$$

$$\omega_B = Pi_B + Qj_B + Rk_B \tag{3.2}$$

$$F_B = Xi_B + Yj_B + Zk_B \tag{3.3}$$

$$M_B = Li_B + Mj_B + Nk_B \tag{3.4}$$

Whereas

$i_B - j_B - k_B$ are body frame vectors.

3.2 Derivation of the equations of motion

The plane motion equations are derived from Newton's second law as follows:

$$F_B = \frac{d}{dt}(mV_B)|_i \tag{3.5}$$

$$M_B = \frac{d}{dt}(H_B)|_i \tag{3.6}$$

Where (i) denotes the frame of inertia, and (B) denotes the frame of the body, while H_B is defined by the following formula:

$$H_B = I_B w_B \tag{3.7}$$

I_B is an inertia matrix and is equal to

$$I_B = \begin{bmatrix} I_{xx} & -I_{xy} & -I_{xz} \\ -I_{yx} & I_{yy} & -I_{yz} \\ -I_{zx} & -I_{zy} & I_{zz} \end{bmatrix} \tag{3.8}$$

By applying Coriolis' theorem to equations 1 and 2, we obtain the following:

$$F_B = \frac{d}{dt}(mV_B)\,|_B + \omega_B \otimes (MV_B) \tag{3.9}$$

$$M_B = \frac{d}{dt}(I_B\omega_B)\Big|_B + \omega_B \otimes (I_B\omega_B) \tag{3.10}$$

By solving equations (3-9) and (3-10) and comparing them with equations (3-3) and (3-4), we find that:

$$X = m(\dot{U} + WQ - VR) \tag{3.11}$$

$$Y = m(\dot{V} + UR - WP) \tag{3.12}$$

$$Z = m(\dot{W} + VP - UQ) \tag{3.13}$$

$$L = \dot{P}I_{xx} - \dot{R}I_{xz} + QR(I_{zz} - I_{yy}) - PQI_{xz} \tag{3.14}$$

$$L = \dot{Q}I_{yy} + PR(I_{xx} - I_{zz}) + (P^2 - R^2)I_{xz} \tag{3.15}$$

$$N = \dot{R}I_{zz} - \dot{P}I_{xz} + PQ(I_{yy} - I_{xx}) - QRI_{xz} \tag{3.16}$$

3.3 Frames Transformation

Equations (3-11) to (3-16) describe the movement of the plane in relation to the frame of the body. Therefore, to relate this movement with respect to the reference frame (Inertial frame), it is necessary to determine the direction of the body frame with respect to the reference frame achieved by using the method of Euler's angles. This defines transitions from one frame to another [8]. The conversion process in this way depends on the sequence of rotations of the axes with each other as follows:

- Rotate the axes of the XE, YE, ZE reference frame in azimuthal angle Ψ around the ZE axis to obtain the X1, Y1, Z1 center axles.
- Rotate the X1, Y1, Z1 axes with an elevation angle around the Y1 axis to get the X2, Y2, Z2 axes.
- Rotate the X2, Y2, Z2 axes with bank angle around the X2 axis to obtain the axes of the reference frame XB, YB, ZB.

This sequence of rotations starts from the reference frame all the way to the body frame. With the help of Fig. 2.3 and the rule of cosine, the individual rotation matrices can be written as follows: -

$$B_\Psi = \begin{bmatrix} C_\Psi & S_\Psi & 0 \\ -S_\Psi & C_\Psi & 0 \\ 0 & 0 & 1 \end{bmatrix} \rightarrow yaw - rotatain \tag{3.17}$$

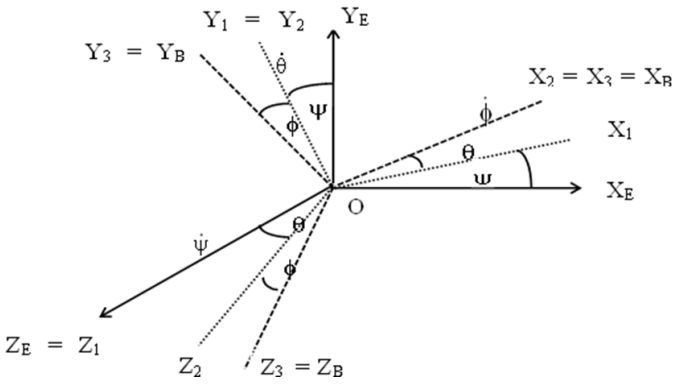

Figure 3.3: Sequence of rotations of axes

$$B_\Theta = \begin{bmatrix} C_\Theta & 0 & -S_\Theta \\ 0 & 1 & 0 \\ S_\Theta & 0 & C_\Theta \end{bmatrix} \rightarrow pitch - rotatain \tag{3.18}$$

$$B_\Phi = \begin{bmatrix} 1 & 0 & 0 \\ 0 & C_\Phi & S_\Phi \\ 0 & -S_\Phi & C_\Phi \end{bmatrix} \rightarrow Roll - rotatain \tag{3.19}$$

If we denote the matrix of total transformations by symbol B, which can be formed from individual matrices as follows

$$\mathbf{B} = B_\Phi B_\Theta B_\Psi \tag{3.20}$$

$$\mathbf{B} = \begin{bmatrix} 1 & 0 & 0 \\ 0 & C_\Phi & S_\Phi \\ 0 & -S_\Phi & C_\Phi \end{bmatrix} \times \begin{bmatrix} C_\Theta & 0 & -S_\Theta \\ 0 & 1 & 0 \\ S_\Theta & 0 & C_\Theta \end{bmatrix} \times \begin{bmatrix} C_\Psi & S_\Psi & 0 \\ -S_\Psi & C_\Psi & 0 \\ 0 & 0 & 1 \end{bmatrix} \tag{3.21}$$

Whereas:-

$\boldsymbol{C}_i$ Denotes the cosine of an angle $\cos(i)$

$\boldsymbol{S}_i$ Denotes the sine of the angle $\sin(i)$

3.4 External forces and momentum affecting the plane

The effect of these forces and momentum is as follows:

1. Lift effect.
2. Thrust effect.
3. Weigh effect.

3.5 Aerodynamic model

They are modeled as follows:

Axial force (disability)

$$X_a = qsC_x \tag{3.22}$$

Lateral Force

$$Y_a = qsC_y \tag{3.23}$$

Natural Forces (Lifting)

$$Z_a = qsC_z \tag{3.24}$$

Torque

$$L_a = qsbC_L \tag{3.25}$$

Lifting torque

$$M_a = qs\bar{c}C_M \tag{3.26}$$

Yaw torque

$$N_a = qsbC_N \tag{3.27}$$

3.5.1 Propulsive Model

There are several types of propulsion systems used in the aviation industry. In this research, a single engine located in the middle of the plane was used, so that the thrust and torque of the engine were modeled as follows:

$$F_p = \frac{4}{\Pi^3}\rho R^4 \Omega^2 C_T \tag{3.28}$$

$$M_p = \frac{4}{\Pi^3} R^5 \Omega^2 C_P \tag{3.29}$$

3.5.2 Gravitation Model

It is known that the force of gravity acts at the center of gravity of the aircraft. C.g. Since the plane's center of gravity corresponds to the center of mass, therefore the force of gravity will not generate torque around the plane [9], and therefore the force of gravity can be written as follows

$$\begin{bmatrix} X_G \\ Y_G \\ Z_G \end{bmatrix} = \mathbf{B} \begin{bmatrix} 0 \\ 0 \\ mg \end{bmatrix} \tag{3.30}$$

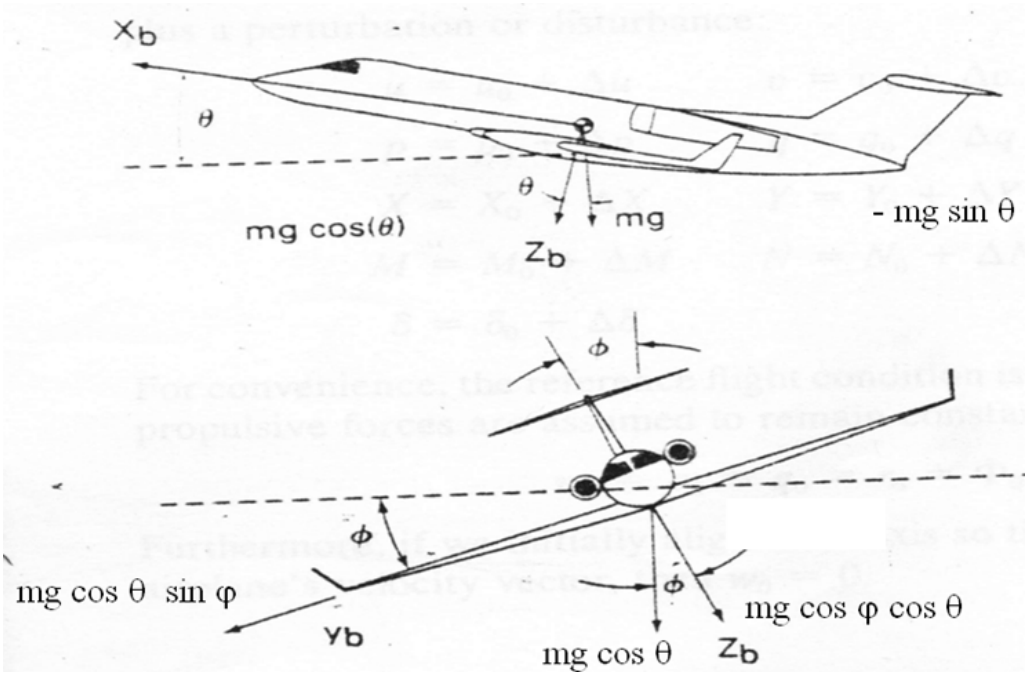

Figure 3.4: the force of gravity acting on the plane

Substituting in the transformation matrix B, we get the following:

$$\begin{bmatrix} X_G \\ Y_G \\ Z_G \end{bmatrix} = \begin{bmatrix} -mg\sin\theta \\ mg\cos\theta\sin\phi \\ mg\cos\theta\cos\phi \end{bmatrix} \tag{3.31}$$

$$L_G = M_G = N_G = 0 \tag{3.32}$$

3.6 Kinematic Equations

The orientation of the aircraft with respect to the frame inertia is determined by the Euler angles. To understand this purpose, an angular velocity vector writes a ratio of Euler angles as follows

$$\omega_B = \dot{\phi} i_\phi + \dot{\theta} j_\theta + \dot{\psi} k_\psi \tag{3.33}$$

After solving the unit vectors in the frame of the body, the Euler angular velocity is given as follows:

$$\begin{bmatrix} \dot{\phi} \\ \dot{\theta} \\ \dot{\psi} \end{bmatrix} = \begin{bmatrix} 1 & \sin\phi\tan\theta & \cos\phi\tan\theta \\ 0 & \cos\phi & -\sin\phi \\ 0 & \sin\phi\sec\theta & \cos\phi\sec\theta \end{bmatrix} \begin{bmatrix} P \\ Q \\ R \end{bmatrix} \tag{3.34}$$

Whereas:

P , Q , R are taken from the output of the modified plane-linked gyroscope.

3.7 Navigation Equations

The position of the aircraft's center of gravity with respect to the reference frame can be determined using the orthogonal transformation matrix and the position vector as follows:

$$\dot{P}_a = \mathbf{B}^T \begin{bmatrix} U \\ V \\ W \end{bmatrix} \tag{3.35}$$

After performing the operation to substitute the value of the matrix B, we obtain:

$$\begin{bmatrix} \dot{P}_N \\ \dot{P}_E \\ \dot{P}_D \end{bmatrix} = \begin{bmatrix} C_\psi C_\theta & C_\psi S_\theta S_\phi - S_\psi C_\phi & C_\psi S_\theta S_\phi + S_\psi C_\phi \\ S_\psi C_\theta & S_\psi S_\theta S_\phi + C_\psi C_\phi & S_\psi S_\theta C_\phi - C_\psi S_\phi \\ -S_\theta & C_\theta S_\phi & C_\theta C_\psi \end{bmatrix} \begin{bmatrix} U \\ V \\ W \end{bmatrix} \tag{3.36}$$

The dynamic equations for previous plane movement can be summarized as follows:

Force Equations

$$X_A + X_G + X_T = m(\dot{U} + WQ - VR) \tag{3.37}$$

$$Y_A + Y_G + X_T = m(\dot{V} + UR - WP) \tag{3.38}$$

$$Z_A + Z_G + Z_T = m(\dot{W} + VP - UQ) \tag{3.39}$$

Moment Equations

$$L_A + L_G + L_T = \dot{P}I_{xx} + QR(I_{zz} - I_{yy}) - (\dot{R} + PQI)I_{xz} \tag{3.40}$$

$$M_A + M_G + M_T = \dot{Q}I_{yy} + PR(I_{xx} - I_{zz}) - (P^2 + R^2)I_{xz} \tag{3.41}$$

$$N_A + N_G + N_T = \dot{R}I_{zz} - \dot{P}I_{xz} + PQ(I_{yy} - I_{xx}) - QRI_{xz} \tag{3.42}$$

Kinematic Equations

$$\begin{bmatrix} \dot{\phi} \\ \dot{\theta} \\ \dot{\psi} \end{bmatrix} = \begin{bmatrix} 1 & \sin\phi\tan\theta & \cos\phi\tan\theta \\ 0 & \cos\phi & -\sin\phi \\ 0 & \sin\phi\sec\theta & \cos\phi\sec\theta \end{bmatrix} \begin{bmatrix} P \\ Q \\ R \end{bmatrix} \tag{3.43}$$

Navigation Equations

$$\begin{bmatrix} \dot{P}_N \\ \dot{P}_E \\ \dot{P}_D \end{bmatrix} = \begin{bmatrix} C_\psi C_\theta & C_\psi S_\theta S_\phi - S_\psi C_\phi & C_\psi S_\theta S_\phi + S_\psi C_\phi \\ S_\psi C_\theta & S_\psi S_\theta S_\phi + C_\psi C_\phi & S_\psi S_\theta C_\phi - C_\psi S_\phi \\ -S_\theta & C_\theta S_\phi & C_\theta C_\psi \end{bmatrix} \begin{bmatrix} U \\ V \\ W \end{bmatrix} \tag{3.44}$$

3.8 Linear Model

It is obtained by converting the non-linear model (equations) into a linear model around a specific operating point linked to specific flight conditions. The information obtained from this point is known by the audit data in Trim data, which are used as reference values for the conversion process. There are several algorithms to complete the Trim process, including the analytical including numerical. In this paper, the transformation process is performed using Linmod function, which is one of the numerical algorithms available in Matlab environment. This function is used as follows:

$$\begin{bmatrix} A & B & C & D \end{bmatrix} = Linmode(G, X_T) \tag{3.45}$$

Whereas $A\ B\ C\ D \equiv$ the linear state space model . $G \equiv$ the nonlinear system Simulink model. $X_T \equiv$ trim data vector. In general, the working point for steady wing level flight and each state vector was chosen as follows:

The output vector is as follows

$$y = \begin{bmatrix} x_e & y_e & z_e & \phi & \theta & \psi & V_T & \beta & \alpha \end{bmatrix}^T \tag{3.46}$$

The non-linear model of the plane around at flight conditions is as follows:

Table 3.1: The non-linear model of the plane around at flight conditions

Operating Point	Airspeed	Altitude	Bank Angle	Fuel Mass	Flap setting
1	23	200	0	2	0
2	25	500	0	1.5	0
3	30	1000	0	1	0

After the conversion has been completed, the linear model of the plane is as follows:

Linear model - Operating Point (1)

Table 3.2: Linear model - Operating Point (1)

STATES(x_{trim})	INPUT (δ_{trim})	OUTPUT (y_{trim})
$x_e = 0$	δ_e = -0.1088	$x_e = 0$
$y_e = 0$	δ_a = -0.0084	$y_e = 0$
z_e = -200m	δ_r =-0.0010	z_e =-200m
ϕ = -0.02deg	$\delta_t = 0.4847$	ϕ = -0.02deg
$\theta = 3.77$deg		$\psi = 0.02$deg
$\psi = 0.02$deg		V_T =23 m s
$u = 22.95$		$\theta = 3.77$deg
v =0.01		$\beta = 0.02$deg
$w = 1.51$		$\alpha = 3.77$deg
p = 0.00		
q = 0.00		
r = 0.00		
fuelmass =2kg		
engin speed =4812		

Longitudinal Model

$$\begin{bmatrix} \dot{u} \\ \dot{w} \\ \dot{q} \\ \dot{\theta} \end{bmatrix} = \begin{bmatrix} -0.2197 & 0.6002 & -1.4884 & -9.7965 \\ -0.5820 & -4.1201 & 22.4025 & -0.6461 \\ 0.4823 & -4.5281 & -4.7508 & 0 \\ 0 & 0 & 1.0000 & 0 \end{bmatrix} \begin{bmatrix} u \\ w \\ q \\ \theta \end{bmatrix} + \begin{bmatrix} 0.3246 & 0 \\ -2.1518 & 0 \\ -29.8191 & 0 \\ 0 & 0 \end{bmatrix} \begin{bmatrix} \delta_e \\ \delta_t \end{bmatrix} \tag{3.47}$$

Linear model - Operating point (2)

Table 3.3: Linear model - Operating Point (2)

STATES (x_{trim})	INPUT (δ_{trim})	OUTPUT (y_{trim})
$x_e = 0$	δ_e = -0.0399	$x_e = 0$
$y_e = 0$	δ_a = -0.0082	$y_e = 0$
z_e = -500m	δ_r = -0.0010	z_e = -500m
ϕ = -0.02deg	δ_t = 0.6300	ϕ = -0.02deg
θ = 2.67deg		ψ =-0.2deg
ψ = -0.2 *deg*		V_T =23 m s
u = 22.95		θ = 2.67deg
v =0.01		β = 0.02deg
w = 1.16		α = 2.67deg
p = 0.00		
q = 0.00		
r= 0.00		
fuelmass =1.5kg		
engine speed =5187		

Longitudinal model

$$\begin{bmatrix} \dot{u} \\ \dot{w} \\ \dot{q} \\ \dot{\theta} \end{bmatrix} = \begin{bmatrix} -0.2440 & 0.5274 & -1.1452 & -9.8085 \\ -0.5927 & -4.5599 & 24.3659 & -0.4575 \\ 0.4052 & -4.6753 & -5.0142 & 0 \\ 0 & 0 & 1.0000 & 0 \end{bmatrix} \begin{bmatrix} u \\ w \\ q \\ \theta \end{bmatrix} + \begin{bmatrix} 0.3556 & 0 \\ -2.5995 & 0 \\ -34.2274 & 0 \\ 0 & 0 \end{bmatrix} \begin{bmatrix} \delta_e \\ \delta_t \end{bmatrix} \tag{3.48}$$

Linear model - Operating point (3)

Table 3.4: Linear model - Operating Point (3)

STATES (x_{trim})	INPUT (δ_{trim})	OUTPUT (y_{trim})
$x_e = 0$	δ_e = -0.0393	$x_e = 0$
$y_e = 0$	δ_a = -0.0081	$y_e = 0$
z_e = -500m	δ_r = -0.0009	z_e = -500m
ϕ = -0.02deg	δ_t = 1.1058	ϕ = -0.02deg
θ = 1.02deg		ψ =0.53deg
ψ = -0.53deg		V_T =23 m s
u = 22.99		θ = 1.02deg
v =0.01		β = 0.02deg
w = 0.53		α = 1.02deg
p = 0.00		
q = 0.00		
r = 0.00		
fuelmass =1kg		
engin speed =6199		

Longitudinal model

$$\begin{bmatrix} \dot{u} \\ \dot{w} \\ \dot{q} \\ \dot{\theta} \end{bmatrix} = \begin{bmatrix} \text{-0.2652} & 0.4647 & \text{-0.8736} & \text{-9.7995} \\ \text{-0.3639} & \text{-4.9312} & 26.3276 & \text{-0.3226} \\ 0.3435 & \text{-4.7274} & \text{-5.1566} & 0 \\ 0 & 0 & 1.0000 & 0 \end{bmatrix} \times \begin{bmatrix} u \\ w \\ q \\ \theta \end{bmatrix} + \begin{bmatrix} 0.2482 & 0 \\ \text{-3.0652} & 0 \\ \text{-37.5976} & 0 \\ 0 & 0 \end{bmatrix} \times \begin{bmatrix} \delta_e \\ \delta_t \end{bmatrix} \tag{3.49}$$

3.9 The process of transient analysis of the mathematical model

3.9.1 Introduction

The process of transient analysis of the mathematical model is carried out in order to know the stability characteristics related to longitudinal movement pattern, using the matrix transformation technique known as the modal decomposition technique.

3.9.2 Modal Decomposition

It is one of the linear algebra techniques that are used to convert a normal state space model into another form known as a modal form. The purpose of this analysis is to deepen and increase the understanding of the dynamic behavior (transient response) of an aircraft. In addition to that, the possibility of seeing and separating the state variables affecting each of the natural plane movement patterns.

The modal transformation technique boils down to the following:

Consider the model for the normal state space of the system as follows:

$$\dot{x} = Ax + B\delta \tag{3.50}$$

$$y = Cx + D\delta \tag{3.51}$$

Let z be a new state vector defined as

$$Z = Tx \tag{3.52}$$

Where T is an eigenvector transformation matrix.

$$\dot{Z} = A_1 Z + B_1 \delta \tag{3.53}$$

$$y = C_1 Z + D_1 \delta \tag{3.54}$$

where:

$A_1 = TAT^{-1}$ is the modal state (eigenvalue) matrix.

$C_1 = CT^{-1}$ is the modal control matrix

$D_1 = D$ is the direct matrix

As follows the modal form by taking the operating point (1) and transforming the longitudinal form the:

Eigenvalues Matrix: (longitudinal dynamics)

$$A_{1l} = \begin{bmatrix} -4.4343 + 10.1013i & & & \\ & -4.4343 + 10.1013i & & \\ & & -0.1117 + 0.5966i & \\ & & & -0.1117 + 0.5966i \end{bmatrix} \tag{3.55}$$

Wheres

first and second column≡ Short Period

third and fourth column ≡ Long Period (Phugoid)
Eigenvectors Matrix:

$$T_l = \begin{bmatrix} -0.0480 + 0.0025i & -0.0480 + 0.0025i & -0.9951 & -0.9951 \\ 0.9100 & 0.9100 & -0.0673 + 0.0042i & -0.0673 + 0.0042i \\ -0.0130 + 0.4099i & -0.0130 + 0.4099i & -0.0376 + 0.0007i & -0.0376 + 0.0007i \\ 0.0345 - 0.0139i & 0.0345 - 0.0139i & 0.0126 + 0.0607i & 0.0126 + 0.0607i \end{bmatrix} \tag{3.56}$$

Wheres
first and second column≡ Short Period
third and fourth column ≡ Long Period (Phugoid)
Control Modal Matrix :

$$B_{1l} = \begin{bmatrix} 29.7601 + 0.0062i \\ 0.3443 - 0.1260i \\ 1.1463 + 0.9937i \\ -0.4378 - 1.8456i \end{bmatrix} \tag{3.57}$$

Whereas:
A_{1l} Longitudinal auxiliary state matrix.
B_{1l} Longitudinal auxiliary control matrix.
T_l The Eigenvector Longitudinal Matrix.

3.9.3 Transient Analysis

The longitudinal matrix of Eigenvalues shows that there are two sets of compound poles, which can be divided according to the frequencies into:

1. The low frequency group represents the long period (phugoid) mode.
2. high frequency group is the short period mode.

3.9.3.1 Long Period Mode (Phugoid)

The stability characteristics related to this pattern are summarized in Table (3-3)

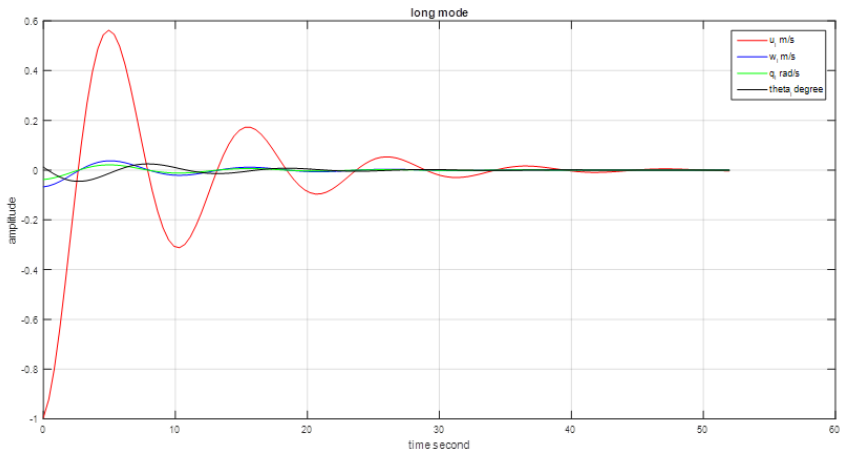

Figure 3.5: The transient response to the long period pattern

Table 3.5: Characteristics of the long period pattern

Mode	Eigenvalue	DR	NF	Period second
Phugoid Mode	-0.0549 ± 0.569i	0.0961	0.5716	11.0430

When the longitudinal state matrix is excited with the real parts of the Eigenvectors corresponding to the Eigenvalues of the long period pattern, its transient response is as shown in Figure (3-5).

From the figure it is noted that this pattern is governed by axial velocity perturbations with some small changes in normal velocity, inclination rate, and inclination angle. This pattern is subdued by the force of axial obstruction.

3.9.3.2 Short Period Mode

The stability characteristics related to this pattern are summarized in the following table:

Table 3.6: Characteristics of the short period pattern

Mode	Eigenvalue	DR	NF	Period second
Short Period	-4.4336 ± 10.1007i	0.4019	11.0314	0.6220

The table above shows the following:

1. The pattern is stable (negative Eigenvalues).

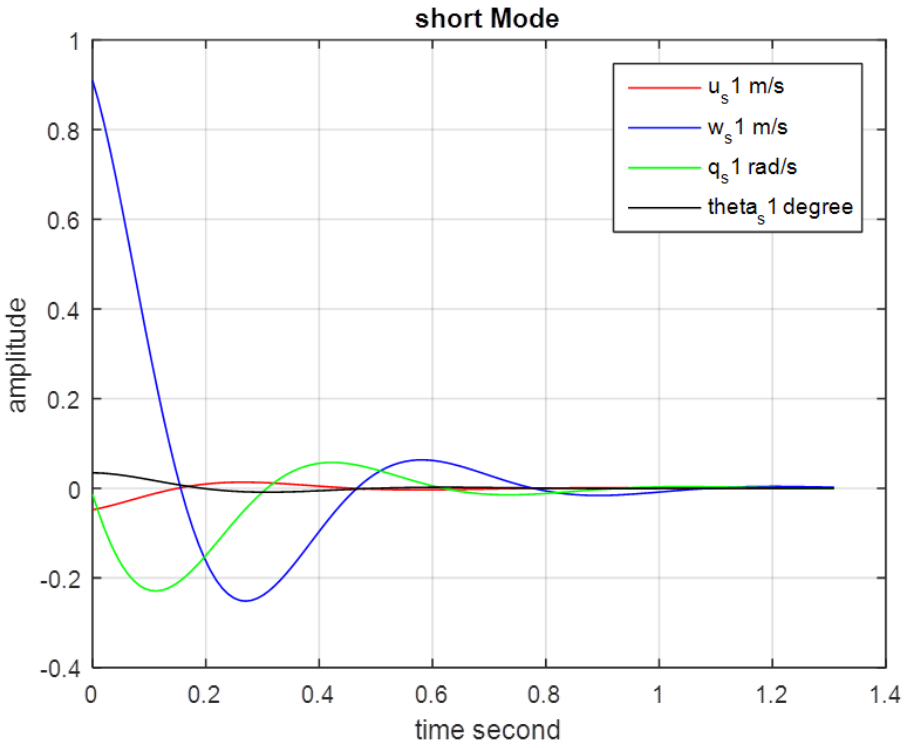

Figure 3.6: The transient response to the short period pattern

2. It has a high frequency.

3. Has good damping.

The transient response to this pattern appears when the state matrix is excited by the longitudinal motion of the real parts of the Eigenvector matrix corresponding to the Eigenvalues of the short period pattern as in the figure (3.6).

From the figure (3.6) it is noted in this pattern that it is governed by the natural speed and the lift rate.

Chapter Four
Control system design

4.1 Introduction

The control system on the plane works to direct the plane by changing its path to the desired path.

4.2 Flight Control Systems

It is divided into the following:

4.2.1 Stability augmentation system (SAS)

It is used to eliminate high-frequency patterns by adding artificial damping to the system. And it controls the signal path between the output and the actuators [10].

4.2.2 Control augmentation system (CAS)

It is used to provide the pilot with a special type of response to reference input. Enhances pilot strength to make flying more accurate and easy. It controls the forward path of the block diagram of the flight control system [11].

4.2.3 Autopilot

It is a control system used to steer an aircraft without the assistance of a pilot. It is used to control low-frequency patterns, in addition to helping the pilot accomplish many routine tasks. It is classified into the following types:

Single-axis autopilot: This is used to control aircraft in the axis of rotation only, such as the ”wing levelers”.

Two-axis autopilot: This is used to control the aircraft in the lifting axis in addition to rotating.

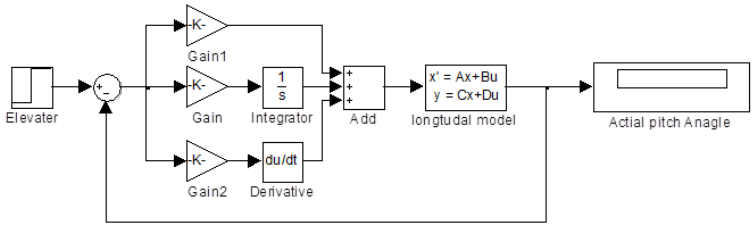

Figure 4.1: Block diagram for control pitch angle control

Three-axis autopilot: Adds control in the yaw axis and is not required on many small aircraft.

In order for the response to be acceptable, you must achieve the following:

1. The system must be stable, that is, its output for any income stabilizes at a specific value.
2. The stable output should be equal to or close to the reference input (steady-state error is very small).
3. The transient performance must be acceptable so that the output follows the reference input at all moments.
4. The system must be of little sensitivity to the changes that occur to some components of the system.

In this research, we will design an autopilot system that stabilizes the aircraft in the longitudinal channel.

4.3 Pitch Angle Control

This type of control system works to stabilize the plane in the longitudinal channel, by feeding the angle of inclination back to the elevator, as in Figure (4-1)

4.4 Design control system for longitudinal movement:

From equation (3-48) it is clear that the linear model of longitudinal motion of the fourth order does not give a deep understanding of the dynamic behavior of the aircraft. In addition, the autopilot will also be of the fourth order, and this leads to somewhat complicating the design process in addition to some limitations in practical applications [12]. As explained in the previous chapter, the longitudinal dynamics usually consist of a slow pattern, known as a phugoid, and a fast pattern, known as a short period. Accordingly, the linear model of the longitudinal channel can be reduced either to an approximate short pattern or to an approximate long pattern.

4.5 Linear approximate model

• To extract the slow mode pattern, the lateral velocity (W) and the lift angle ratio must be equal to zero.

$w = q = 0$

• To extract the quick model, both the axial velocity (U) and the angle of inclination must be equal to zero.

$U = \theta = 0$

Therefore, the approximate models for each of the slow and fast patterns are as follows:

$$As = \begin{bmatrix} -4.1201 & 22.4025 \\ -4.5281 & -4.5207 \end{bmatrix} Bs = \begin{bmatrix} -2.1518 \\ -29.8291 \end{bmatrix} \longrightarrow (short - period) \tag{4.1}$$

$$Ap = \begin{bmatrix} -0.2197 & -9.7965 \\ 0 & 0 \end{bmatrix} Bp = \begin{bmatrix} -0,3246 \\ 0 \end{bmatrix} \longrightarrow (phugoid - period) \tag{4.2}$$

The Eigenvalue for the fast pattern for both the macro and approximate models are given as follows

$\lambda s_{1,2}$ = -4.4343 ±10.1013i $\longmapsto$ (Full-order)

$\lambda s_{1,2}$ = -4.4355 ± 10.0668i $\longmapsto$ (Approximate)

And also the Eigenvalue for slow pattern is as follows

$\lambda p_{1,2}$ = -0.1117 ± 0.5966i $\longmapsto$ (Full-order)

$\lambda p_{1,2}$ = -0.2197 $\longmapsto$ (Approximate)

By calculating Time of half Amplitude, we get the following

Time of half amplitude

$t_{\frac{1}{2}} = \frac{0.69}{|-4.4343|} = 0.1556051689777809$ [Sec] (Full-order) (Short period)

$t_{\frac{1}{2}} = \frac{0.69}{|-4.4355|} = 0.15556307067974$ [Sec] (Approximate) (Short period)

$t_{\frac{1}{2}} = \frac{0.69}{|-0.1117|} = 6.177260519247986$ [Sec] (Full-order) (Phugoid)

$t_{\frac{1}{2}} = \frac{0.69}{|-0.2197|} = 3.140646335912608$ [Sec] (Approximate) (Phugoid)

Period of half amplitude

$P_r = \frac{2\pi}{10.1013} = 0.1980$ [Sec] (Full-order) (Short period)

$P_r = \frac{2\pi}{10.0668} = 0.1987$ [Sec] (Approximate) (Short period)

$P_r = \frac{2\pi}{0.5966} = 10.5317$ [Sec] (Full-order) (phugoid)

$P_r = \frac{2\pi}{0} = \infty$ [Sec] (Approximate) (phugoid)

Table 4.1: A comparison between fast and slow patterns

	Full-order	Reduced-order	Difference
Short period	$t_{\frac{1}{2}} = 0.1556051689777809$	$t_{\frac{1}{2}} = 0.15556307067974$	0.042 ٪
	$P_r = 0.1980$	$P_r = 0.1987$	0.336 ٪
Phugoid	$t_{\frac{1}{2}} = 6.177260519247986$	$t_{\frac{1}{2}} = 3.140646335912608$	49.159 ٪
	$P_r = 10.5317$	$P_r = \infty$	NAN

From the above table, it is clear that the approximate fast pattern model is closer to the total pattern, and therefore it will be used in the design of the longitudinal automatic control system instead of the total model of the longitudinal channel.

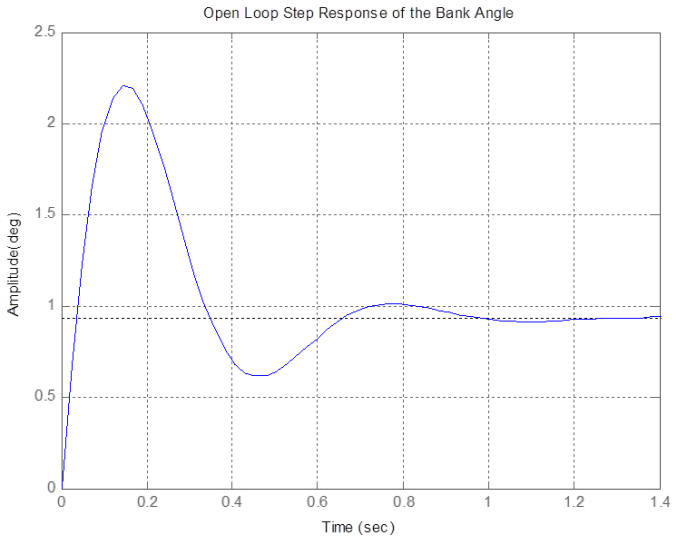

Figure 4.2: The open loop response

4.5.1 Open loop response

To find the open-loop response, the approximate longitudinal model (short period pattern model) was excited using the step function. The simulation results are illustrated in Fig. (4-2) and the specifications of the open loop system are illustrated in Table (4-2).

Table 4.2: Performance specifications for the short period

System Settings	Rise Time	Peak Time	Settling Time	Overshoot	SSE
Open Loop	0.0281	0.143	0.914	137	0.065

4.5.2 Finding control for longitudinal motion

The geometric position of the roots method was used to draw the geometric position of the roots of the open loop system Fig (4-3), and then a number of points were randomly selected as in Table (4-3).

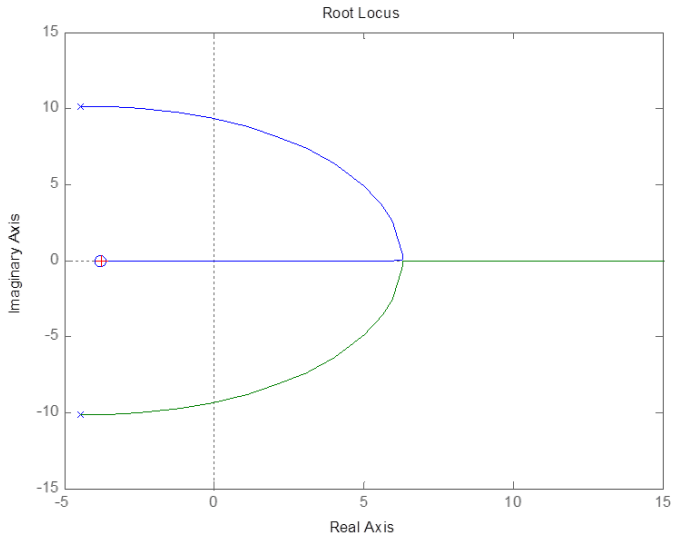

Figure 4.3: The locus of roots

Table 4.3: Performance specifications for gain values

Selected point	Kc	Wc	RT	PT	ST	Overshoot	SSE
-2.891-0.0466i	3.8498	0.04660	0.0082	0.0213	0.1039	44.4389	0
-3.4123-0.0466i	8.9449	0.0466	0.0053	0.0133	0.0526	32.7536	0
-3.5545-0.0466i	14.0727	0.0466	0.0042	0.0102	0.0327	26.1569	0
-3.6493-0.0466i	22.5839	0.0466	0.0033	0.0085	0.0265	20.1119	0
-3.6967-0.0466i	31.8428	0.0466	0.0029	0.0073	0.0222	16.114	0
-3.7915-0.0466i	73.1930	0.0466	0.0021	0.0054	0.0124	8.6561	0
-3.8389-0.0466i	52.3626	0.0466	0.0024	0.0063	0.0132	11.2530	0

From the table, we find that the point (-3.7915-0.0466i) selected on the engineering position is the one that achieves the best level of the plane's performance and the response of the longitudinal channel of the front controller is as in Figure (4-4).

4.6 Controller Evaluation

The controller is evaluated from the standpoint of neglected dynamics by deleting the model represented by the operating point (1) and compensating for it by the two models at points (2) (3). After compensation, it was found that the controller could maintain a steady semi-response, which indicates its

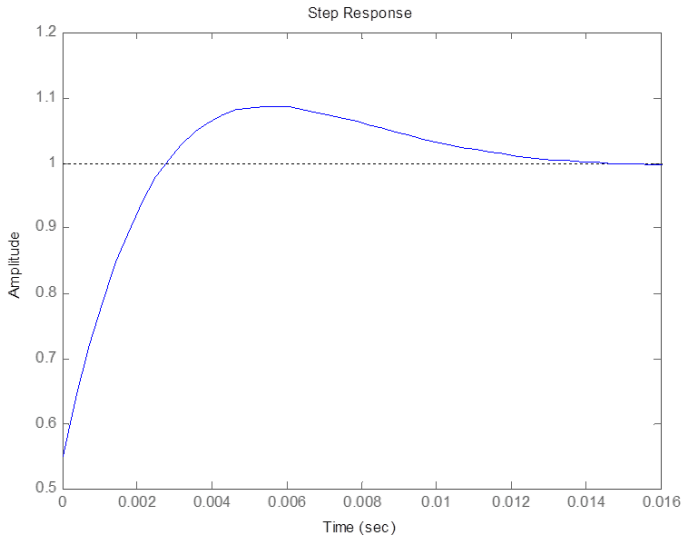

Figure 4.4: System response to forward feeding gain

durability.

4.7 Comparison between controller and PID controller:

The comparison of the controller between a preset controller and a PID controller that was calculated in this project for longitudinal movement is shown in the table(4-4).

Table 4.4: Comparison of the controller between a preset controller and a PID controller

Controller	Rise Time	Peak Time	Settling Time	Overshoot	SSE
P	0.008	0.0347	0.467	13	0.849
PID	0.0021	0.0054	0.0124	8.6561	0

Chapter Five
Conclusion and Recommendations

5.1 Conclusions

In this paper, an integral differential proportional controller was designed to control the movement of the aircraft in both the longitudinal and lateral channels by using winches and ailerons. Because controlling aircraft in general and drones in particular needs a system with a fast response and high stability, as the slightest error or delay in sending or implementing control orders in the plane can lead to the aircraft losing its stability and thus to its downfall and crash, or at least. Failure to fulfill its mission assigned to it.

5.2 Recommendations

The model to be used in this research is a hypothetical model. I recommend using the real model that will be extracted .

The synthesis techniques used in this paper are complex techniques that depend on trial and error and require a lot of time to reach the best results. It is better to use self-tuning techniques.

.

Bibliography

[1] I. Moir and A. Seabridge, *Design and development of aircraft systems*. John Wiley & Sons, 2012, vol. 67.

[2] R. Austin, *Unmanned aircraft systems: UAVS design, development and deployment*. John Wiley & Sons, 2011, vol. 54.

[3] L. Romanenko, A. Romanenko, and G. Samarova, "Aircraft longitudinal control without a pitch command in the autopilot," *Russian Aeronautics (Iz VUZ)*, vol. 57, no. 4, pp. 361–367, 2014.

[4] A. K. Singh and R. Dahiya, "Design and modeling of controllers for aircraft pitch contol movement," *ijecs*, 2016.

[5] M. Gopal and I. Nagrath, *Control systems engineering*. Wiley Eastern, 1976.

[6] N. S. Nise, *Control systems engineering*. John Wiley & Sons, 2020.

[7] K. Georgieva and V. Serbezov, "Mathematical model of aircraft ground dynamics," in *2017 International Conference on Military Technologies (ICMT)*. IEEE, 2017, pp. 514–519.

[8] D. Hinrichsen and A. J. Pritchard, *Mathematical systems theory I: modelling, state space analysis, stability and robustness*. Springer Science & Business Media, 2011, vol. 48.

[9] J. Durbin and S. J. Koopman, *Time series analysis by state space methods*. Oxford university press, 2012.

[10] O. Katsuhiko, *Modern control engineering*, 2010.

[11] P. Pounds, R. Mahony, P. Hynes, and J. M. Roberts, "Design of a four-rotor aerial robot," in *The Australian Conference on Robotics and Automation (ACRA 2002)*, 2002, pp. 145–150.

[12] J. Siddall, "Controls," in *Mechanical Design*. University of Toronto Press, 2019, pp. 35–39.

Appendix A

A.1 Transient analysis of longitudinal motion

```
clc
%% longitudenal Channel
% Enter the Jacopian matrices for the longitudenal channel for the operating
% point1 described by the following data:
% H=200(m), Va=23 (m/s), bank angle=0(deg),flap setting=0(frac),fuel
% mass=2(kg)
Al=[-0.2197    0.6002   -1.4881   -9.7969
-0.5820   -4.1207   22.4024   -0.6460
0.4823   -4.5286   -4.7515         0
0         0    1.0000         0 ];
%control matrix
Bl=[0.3246 -2.1518 -29.8191 0]';
%output matrix
Cl=[0 0 0 1];
%direct matrix
Dl=0;
%% calculating the long Mode
sys_l=ss(Al,Bl,Cl,Dl);
[T,A]=eig(Al)

%%extract the real parts eigenvector of the long mode
X_l=real(T(1:4,3));
%initialised the long mode with the real parts eigenvector
[y_l,t_l,x_l]=initial(sys_l,X_l);
%separate long mode states
u_l=[1 0 0 0]*x_l';
w_l=[0 1 0 0]*x_l';
q_l=[0 0 1 0]*x_l';
theta_l=[0 0 0 1]*x_l';
```

```
%plot the long mode states
figure(4)
plot(t_l,u_l,'r',t_l,w_l,'b',t_l,q_l,'g',t_l,theta_l,'k');grid
title('long mode')
ylabel('amplitude')
xlabel('time second')
legend('u_l m/s','w_l m/s','q_l rad/s','theta_l degree')
%% calculating the short Mode
sys_s1=ss(Al,Bl,Cl,Dl);
[V,E]=eig(Al);
%%extract the real parts eigenvector of the short mode
X_s1=real(V(1:4,1));
%initialised the short mode with the real parts eigenvector
[y_s1,t_s1,x_s1]=initial(sys_s1,X_s1);
%separate short mode states

u_s1=[1 0 0 0]*x_s1';
w_s1=[0 1 0 0]*x_s1';
q_s1=[0 0 1 0]*x_s1';
theta_s1=[0 0 0 1]*x_s1';
%plot the short mode states
figure(5)
plot(t_s1,u_s1,'r',t_s1,w_s1,'b',t_s1,q_s1,'g',t_s1,theta_s1,'k');grid
title('short Mode')
ylabel('amplitude')
xlabel('time second')
legend('u_s1 m/s','w_s1 m/s','q_s1 rad/s','theta_s1 degree')
```

A.2 control of longitudinal motion

```
clc
clear all
%% longitudenal Channel
% Enter the Jacopian matrices for the longitudenal channel for the operating
% point1
```

```
A= [-4.1201 22.4025
-4.5281 -4.7508];
B= [-2.1518
-29.8191];
% output matrix
C=[0 1];
% dierct matrix
D=0;
damp(A)
%% plot step response of open loop system
sys_t=ss(A,B,C,D);
figure(1)
step(-sys_t);grid;title('Open Loop Step Response of the Bank Angle');xlabel
%% plot the root locus of the open loop system
figure(2)
rlocus(sys_t);
% find critical gain kc and frequency wc using root locus approach
[kc,polse]=rlocfind(sys_t)

wc=input('enter the value of critical frequnecy wc=')
%% claculate the the tarnsfer function of the PID controller parameters
% Kp,Ki,Kd
tc=wc/(2*pi);
kp=0.6*kc;
ki=kp/(.5*tc);
kd=(.125*tc*kp);
numc=[kd kp ki];
dem=[1 0];
Gpid=tf(numc,dem)
%% calculate the closed loop transfer function of the controlled system
[nump,denump]=ss2tf(A,B,C,D);
Gp=tf(nump,denump)
Gfinal=series(Gp,Gpid)
Gclosed=feedback(Gfinal,-1)
%% plot the step response the closed loop system
figure(4)
```

```
step(-Gclosed)
stepinfo(-Gclosed)
```

Appendix B

B.1 performance data and specification of the Aircraft UAV

Specifications

Weight 15 kg
Wing span 2.9 m
Engine 24 cc PULP, 1.25, fuel injected
Navigation GPS, DGPS
Propeller diameter 0.6 m

Performance

Speed Cruise 20-32 [m/s]; climb 4 [m/s]